2008 Annual SCEC report

Development of semi-analytic models of deformation due to faults in arbitrarily heterogeneous media (PI: Fialko)

Publications and abstracts resulted from this project:

Barbot, S., Y. Fialko and Y. Bock, Postseismic deformation due to the Mw6.0 2004 Parkfield earthquake: Stress-driven creep on a fault with spatially variable rate-and-state friction parameters, J. Geophys. Res. (in revision).

Barbot, S., Y. Fialko and D. Sandwell, Three-dimensional models of elasto-static deformation in heterogeneous media, with application to the Eastern California Shear Zone, Geophys. J. Int. (in press).

Cochran, E., Y.-G. Li, P. Shearer, S. Barbot, Y. Fialko and J. Vidale, Seismic and geodetic evidence for extensive, long-lived fault damage zones, Geology, 37, 315-318, 2009.

Hearn, E. and Y. Fialko, Can compliant fault zones be used to measure absolute stresses in the upper crust?, J. Geophys. Res. (in press).

Barbot, S. and Y. Fialko, Estimation of Relative Contributions of Localized Shear vs Broad Viscous Flow in Postseismic Transients: Case Study of the 1992 Landers and 1999 Hector Mine, California, Earthquakes, Eos, Trans. AGU, 89(53), Suppl., abst. T53C-1969, 2008.

Tong, X., D. T. Sandwell, Y. Fialko and R. J. Mellors, Coseismic Displacement of M8.0 Sichuan Earthquaqke Derived by ALOS Radar Interferometry, Eos, Trans. AGU, 89(53), Suppl., abst. G33C-0715, 2008.

Summary of results:

Models of fault-induced deformation in heterogeneous elastic media.

We developed a semi-analytic iterative procedure for evaluating deformation due to faults in an arbitrary heterogeneous half space, extending the antiplane formulation of *Barbot et al.* (2008) to three dimensions. Spatially variable elastic properties are modeled with equivalent body forces and equivalent surface tractions in a homogeneous elastic medium. Displacement field is obtained in the Fourier domain using semi-analytic Greens' functions. Consider a heterogeneous elastic body Ω containing a shear fracture α with normal $\hat{\mathbf{n}}^\alpha$ and slip $\mathbf{s}^\alpha$. Given the tensor of elastic moduli $\mathbf{C} = \mathbf{C}(\mathbf{x})$, the Cauchy stress

$$\boldsymbol{\sigma} = \mathbf{C} : \boldsymbol{\epsilon}^e \tag{1}$$

where operation : is the double scalar product (for instance if $\mathbf{A}$ and $\mathbf{B}$ are two second-order tensors, then in index notation the product $\mathbf{A} : \mathbf{B}$ is the scalar $A_{ij} B_{ij}$), can be written as follows,

$$\boldsymbol{\sigma} = \mathbf{C} : \boldsymbol{\epsilon} - \mathbf{C} : \boldsymbol{\epsilon}^i \tag{2}$$

where $\boldsymbol{\epsilon}$ is the total strain, and $\boldsymbol{\epsilon}^i$ is the inelastic strain (e.g., due to violation of continuity across the fault surface). The latter can be recognized as the moment density (*Aki and Richards*, 1980; *Shearer*, 1999),

$$\mathbf{m}(\mathbf{x}) = \sum_{\alpha=1}^{n} \mathbf{C}(\mathbf{x}) : \boldsymbol{\epsilon}^\alpha . \tag{3}$$

As elastic properties are spatially variable, the moment density is not necessarily uniform along a dislocation surface. Using Eq. (2), the conservation of momentum for static equilibrium in Ω can be written (*Malvern*, 1969; *Nemat-Nasser and Hori*, 1999)

$$\nabla \cdot (\mathbf{C} : \boldsymbol{\epsilon}) - \nabla \cdot (\mathbf{C} : \boldsymbol{\epsilon}^i) = 0 \tag{4}$$

The second term in Eq. (4) depends upon the distribution and orientation of internal dislocations in Ω. The effect of all internal dislocations may be represented using equivalent body forces (*Burridge and Knopoff*, 1964; *Eshelby*, 1957; *Nemat-Nasser*, 2004)

$$\mathbf{f}(\mathbf{x}) = -\nabla \cdot (\mathbf{C} : \boldsymbol{\epsilon}^i) = \sum_{\alpha=1}^{n} \mathbf{f}^{\alpha}(\mathbf{x}) \tag{5}$$

where

$$\mathbf{f}^{\alpha}(\mathbf{x}) = -\nabla \cdot (\, \mathbf{C} : \mathbf{s}^{\alpha} \otimes \hat{\mathbf{n}}^{\alpha}) \tag{6}$$

is the equivalent body-force density due to an individual dislocation α, and $\mathbf{s}^{\alpha}$ and $\hat{\mathbf{n}}^{\alpha}$ refer to the Burger's vector and the normal direction of dislocation α, respectively. As dislocations may cut across heterogeneous regions, the equivalent body force (6) may not be readily reduced to a double couple.

Our approach consists in using the elastic Green function for a homogeneous medium and in identifying a set of equivalent body forces and equivalent surface tractions that represent the effect of spatial variations in elastic properties.

Figure 1 shows example calculations of surface displacements due to a vertical strike-slip fault in a layered half-space. A comparison with other semi-analytic techniques (e.g., *Wang et al.* (2003)) that are available for simple cases (like the layered half-space) indicates that our method is robust.

We applied our model to investigate the response of compliant zones (CZ) around major crustal faults to coseismic stressing by nearby earthquakes. *Cochran et al.* (2009) showed that the geodetically inferred kilometer-wide compliant fault zones in the Mojave desert (*Fialko*, 2004; *Fialko et al.*, 2002) are also expressed in marked reductions in seismic velocities. The width of the tomographically imaged low velocity zones, as well as the magnitude of velocity reductions were found to be consistent with independent geodetic estimates. Seismic observations reveal the complex structure of the fault damage zones, with large gradients in the effective elastic moduli both laterally and as a function of depth. We constrain the two elastic moduli within the fault zones by comparing model predictions to the InSAR data. Figure 2a shows the observed and modeled LOS displacements along profile A-A'. Profile A-A' crosses over the Calico and the Rodman faults, north of Galway Dry Lake, close to the seismic tomography experiment of *Cochran et al.* (2009). The observed change in polarity in the LOS displacements corresponding to the Hector Mine and Landers coseismic interferograms is an expected signature of the vertical displacement due to a compliant zone, given a reversal in sign of the fault-normal coseismic stress change. The assumed location and thickness of the Calico and Rodman compliant zones are indicated in Figure 2a by gray bands. Solid lines in Figure 2a represent deformation due to our preferred fault zone model, sampled along the respective profiles. Results shown in Figure 2a accurately simulate the 3-D response of closely spaced compliant zones due to the Calico and Rodman faults to coseismic loading, and represent a substantial improvement over the previously published simplified models (e.g., *Fialko et al.*, 2002). Our preferred model for the compliant zone surrounding the Calico fault, north of Galway Dry Lake, implies a 60% reduction in shear modulus and no change in the Poisson's ratio (accompanied by a 60% reduction in the value of the bulk modulus) compared to ambient rocks, in a finite zone 4 km deep and 2.0 km wide, consistent with seismic tomography data (*Cochran et al.*, 2009). Our preferred model for the CZ due to the Rodman fault implies the same elastic moduli reduction, but to a shallower depth of $D = 2.0$ km. These observations suggest pervasive

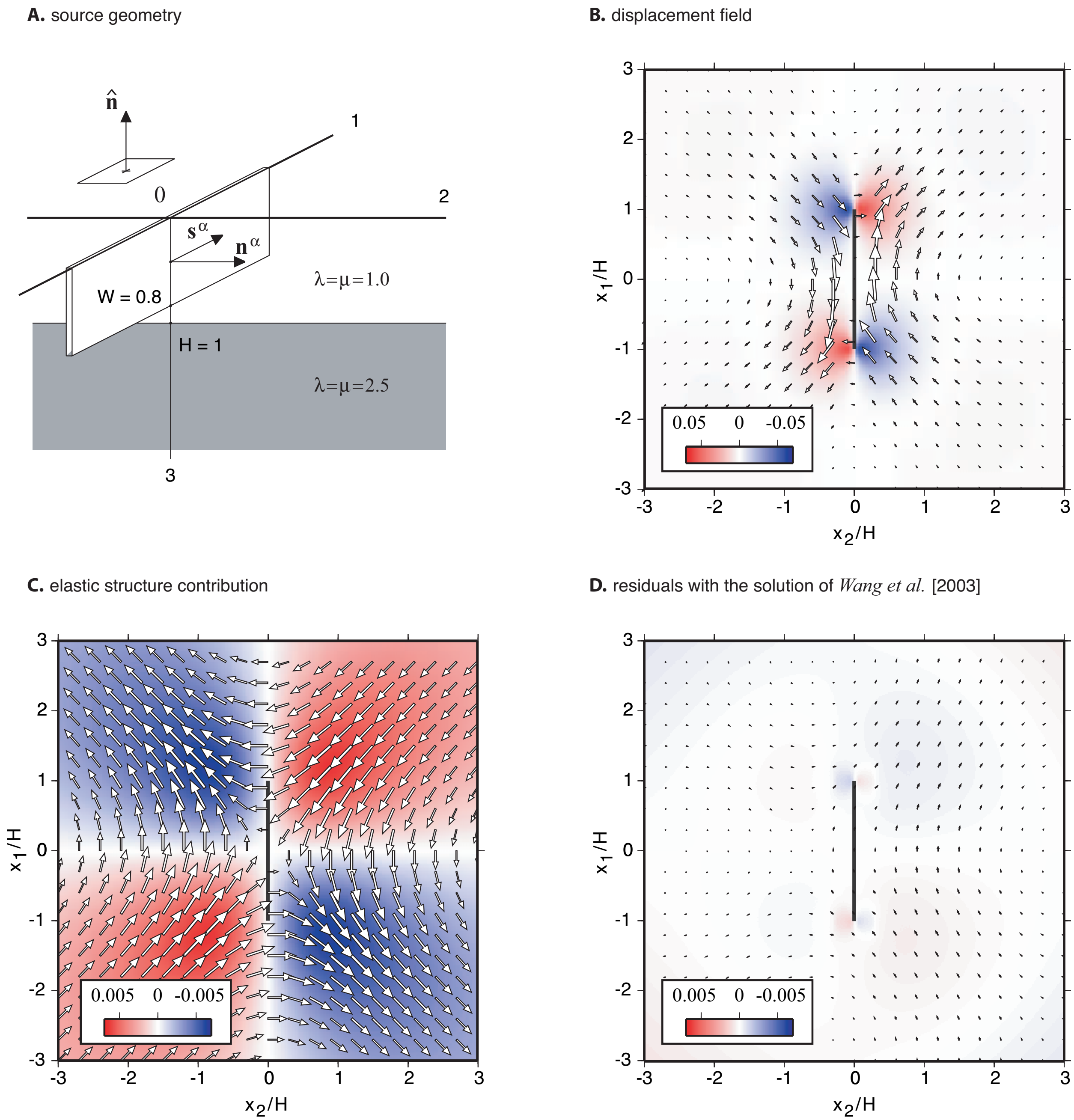

Figure 1: Three-dimensional benchmark. A) A strike-slip fault extending to the Earth's surface. The rigidity in the bottom half space is 2.5 times higher than in the top plate. B) The displacement field at the surface of the half space. C) Difference between the heterogeneous model and the homogeneous solution. D) Difference between our solution and that obtained using the propagator matrix approach of *Wang et al.* (2003).

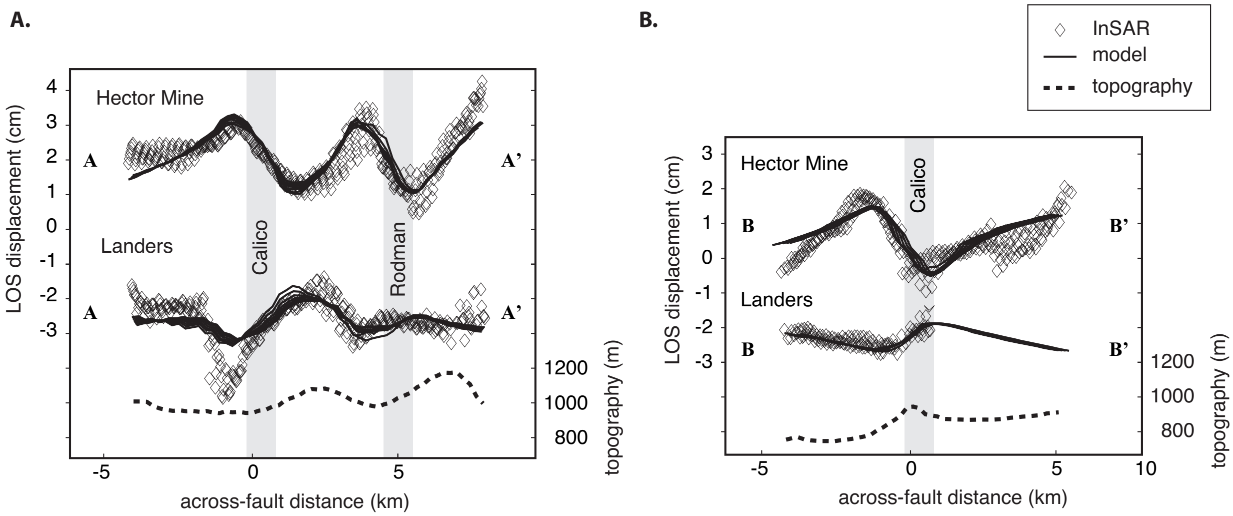

Figure 2: Observed (diamond) and modeled (solid line) LOS displacements from profile A-A' corresponding to the Landers (bottom) and Hector Mine (top) coseismic interferograms North of Galway Dry Lake. B) Observed and modeled LOS residual displacements across a southern segment of the Calico fault (profile B-B'). The continuous curves correspond to forward models from several closely spaced parallel profiles.

and widespread damage around active crustal faults.

Effect of coseismic changes in the fault-zone properties in the presence of gravity and tectonic stress.

Fault-zone trapped wave studies suggested a small reduction in P and S wave velocities along the Johnson Valley Fault caused by the 1999 Hector Mine earthquake (*Vidale and Li*, 2003). This reduction presumably perturbed a permanent compliant structure associated with the fault. The inferred changes in the fault zone compliance may produce a measurable deformation in response to background (tectonic) stresses. This deformation should have the same sense as the background stress, rather than the coseismic stress change.

Hearn and Fialko (2009) investigated how the observed deformation of compliant zones in the Mojave Desert can be used to place limits on the fault zone structure as well as on stresses in the upper crust. We find that the gravitational contraction of the coseismically softened zones dominates over the Poissonian expansion due to the fault-normal stress, unless the compliant fault zones are both shallow and narrow, or essentially incompressible. We prefer the latter interpretation (or related explanations in the discussion section, which relate to material properties) because profiles of LOS displacements across compliant zones cannot be fit by narrow, shallow compliant zones. Strain of the Camp Rock fault zone during the Hector Mine earthquake suggests that background deviatoric stresses are consistent with Mohr-Coulomb theory in the Mojave upper crust. However, with large uncertainties in compliant zone properties and geometry, we cannot estimate Mojave crustal stresses with meaningful precision. As the geometry and elastic properties of compliant zones are better understood, models of coseismic strain may provide important constraints on upper crustal stresses.

Modeling of stress-diven afterslip on a fault with spatially variable frictional proper-

ties.

In *Barbot et al.* (in review) we investigated stress-driven creep on a fault plane following an earthquake (on the same or neighboring fault). We developed a numerical model that evaluates the time-dependent deformation due to coseismic stress changes in an elasto-plastic half-space. Starting with a coseismic slip distribution, we compute the time-dependent evolution of afterslip on a fault plane and the associated displacements at the Earth's surface. We applied our model to study the co- and postseismic deformation due to the M_w6.0 2004 Parkfield, CA earthquake. We produced co- and postseismic slip models by inverting data from an array of 14 continuous GPS stations from the SCIGN network. Kinematic inversions of postseismic GPS data over a time period of 3 years show that afterslip occurred in areas of low seismicity and low coseismic slip, predominantly at depth of $\sim$5 km. Inversions suggest that coseismic stress increases were relaxed by predominantly aseismic afterslip on a fault plane. Kinetics of afterslip is consistent with a velocity-strengthening friction generalized to include the case of infinitesimal velocities.

Our forward calculations of stress-driven afterslip show that the geodetic data are best explained by a rate-strengthening model with frictional parameter $(a - b) = 7 \times 10^{-3}$, on a high end of values observed in laboratory experiments. We also find that the geodetic moment due to creep is a factor of 100 greater than the cumulative seismic moment of aftershocks. The rate of aftershocks in the top 10 km of the seismogenic zone mirrors the kinetics of afterslip, suggesting that post-earthquake seismicity is governed by loading from the nearby aseismic creep. The San Andreas fault around Parkfield is deduced to have large along-strike variations in rate-and-state frictional properties. Velocity strengthening areas may be responsible for the separation of the coseismic slip in two distinct patches and for the ongoing aseismic creep occurring between the patches following the 2004 rupture.

References

Aki, K., and P. G. Richards, *Quantitative Seismology: Theory and Methods, I and II*, 577 pp., W. H. Freeman, San Francisco, Calif., 1980.

Barbot, S., Y. Fialko, and D. Sandwell, Effect of a compliant fault zone on the inferred earthquake slip distribution, *J. Geophys. Res.*, *113*, B06,404, doi:10.1029/2007JB005,256, 2008.

Barbot, S., Y. Fialko, and Y. Bock, Postseismic deformation due to the mw 6.0 2004 parkfield earthquake: Stress-driven creep on a fault with spatially variable rate-and-state friction parameters, *J. Geophys. Res.*, in review.

Burridge, R., and L. Knopoff, Body force equivalents for seismic dislocations, *Bull. Seism. Soc. Am.*, *54*, 1875–1888, 1964.

Cochran, E. S., Y.-G. Li, P. M. Shearer, S. Barbot, Y. Fialko, and J. E. Vidale, Seismic and geodetic evidence for extensive, long-lived fault damage zones, *Geology*, *37*, 315–318, 2009.

Eshelby, J. D., The determination of the elastic field of an ellipsiodal inclusion, and related problems, *Proc. R. Soc. Lond. A*, *241*(1226), 376–396, 1957.

Fialko, Y., Probing the mechanical properties of seismically active crust with space geodesy: Study of the co-seismic deformation due to the 1992 M_w7.3 Landers (southern California) earthquake, *J. Geophys. Res.*, *109*, B03,307, 10.1029/2003JB002,756, 2004.

Fialko, Y., D. Sandwell, D. Agnew, M. Simons, P. Shearer, and B. Minster, Deformation on nearby faults induced by the 1999 Hector Mine earthquake, *Science*, *297*, 1858–1862, 2002.

Hearn, E. H., and Y. Fialko, Can compliant fault zones be used to measure absolute stresses in the upper crust?, *J. Geophys. Res.*, p. (in press), 2009.

Malvern, L. E., *Introduction to the mechanics of a continuum medium*, 713 pp., Prentice-Hall, Englewood Cliffs, NJ, 1969.

Nemat-Nasser, S., *Plasticity. A Treatise on Finite Deformation of Heterogeneous Inelastic Materials*, Cambridge Monographs on Mechanics, Cambridge University Press, 2004.

Nemat-Nasser, S., and M. Hori, *Micromechanics: overall properties of heterogeneous materials*, 2 ed., Elsevier, 1999.

Shearer, P. M., *Introduction to seismology*, Cambridge University Press, New York, 1999.

Vidale, J., and Y. Li, Damage to the shallow Landers fault from the nearby Hector Mine earthquake, *Nature*, *421*, 524–526, 2003.

Wang, R., F. Martin, and F. Roth, Computation of deformation induced by earthquakes in a multi-layered elastic crust - FORTRAN programs EDGRN/EDCMP, *Comp. Geosci.*, *29*, 195–207, 2003.